Extracellular Matrix Abnormalities in the Hippocampus of Subjects with Substance Use Disorder

Jake Valeri[a,b], Charlotte Stiplosek[a], Sinead M. O'Donovan[c], David Sinclair[c], Kathleen A. Grant[d], Ratna Bollavarapu[b], Donna M. Platt[a,b], Craig A. Stockmeier[a,b], Barbara Gisabella[a,b], Harry Pantazopoulos[a,b]

a) Department of Psychiatry and Human Behavior, University of Mississippi Medical Center, Jackson, MS
b) Program in Neuroscience, University of Mississippi Medical Center, Jackson, MS
c) Department of Neuroscience, University of Toledo, Toledo, OH
d) Oregon Primate Research Center, Hillsboro, OR

Address for correspondence:
Harry Pantazopoulos, PhD
Department of Psychiatry and Human Behavior
University of Mississippi School of Medicine
TRC 407
2500 North State St
Jackson, MS 39216, USA
Phone: (601) 815-7983
E-mail: cpantazopoulos@umc.edu

Short title: Extracellular Matrix Abnormalities in Substance Use Disorder

Key words: substance use disorders, major depressive disorder, hippocampus, synaptic signaling, extracellular matrix, perineuronal nets, parvalbumin

ABSTRACT

Contextual triggers are significant factors contributing to relapse in substance use disorders (SUD). Emerging evidence points to a critical role of extracellular matrix (ECM) molecules as mediators of reward memories. Chondroitin sulfate proteoglycans (CSPGs) are a subset of ECM molecules that form perineuronal nets (PNN) around inhibitory neurons. PNNs restrict synaptic connections and help maintain synapses. Rodent models suggest that modulation of PNNs may strengthen contextual reward memories in SUD. However, there is a lack of information regarding PNNs in the hippocampus of people with SUD as well as how comorbidity with major depressive disorder (MDD) may affect PNNs. We used postmortem hippocampal tissues from cohorts of human and nonhuman primates with or without chronic alcohol use to test the hypothesis that PNNs are increased in subjects with SUD. We used to histochemical labeling and quantitative microscopy to examine PNNs, and qRT-PCR to examine gene expression for ECM molecules, synaptic markers and related markers. We identified increased densities of PNNs and CSPG-labeled glial cells in SUD, coinciding with decreased mRNA expression of the ECM protease matrix metalloproteinase 9 (MMP9), and increased expression for the excitatory synaptic marker vesicle associated membrane protein 2 (VAMP2). Similar increases in PNNs were observed in monkeys with chronic alcohol self-administration. Subjects with MDD displayed changes opposite to SUD, and subjects with SUD and comorbid MDD had minimal changes in any of the outcome measures examined. Our findings demonstrate that PNNs are increased in SUD, possibly contributing to stabilizing contextual reward memories as suggested by preclinical studies. Our results also point to a previously unsuspected role for CSPG expression in glial cells in SUD. Evidence for increased hippocampal PNNs in SUD suggests that targeting PNNs to weaken contextual reward memories is a promising therapeutic approach for SUD, however comorbidity with MDD is a significant consideration.

INTRODUCTION

Substance use disorders (SUD) are a group of psychiatric disorders with substantially increased risk of mortality and severe socioeconomic burden affecting approximately 7% of people in the United States annually [1, 2]. SUDs impose a substantial burden of morbidity and mortality, exacerbated by persistently high rates of relapse and treatment failure [3]. Contextual cues associated with drug use are a critical factor contributing to relapse in individuals with SUD and highlight the strength of memory circuits associated with reward processing [3-7]. A growing number of studies indicate a critical role of extracellular matrix molecules (ECM) in the regulation of reward memories [8-17] (for reviews see [18, 19]). Recent gene expression profiling studies demonstrate altered expression of pathways involved in ECM regulation in the dorsolateral prefrontal cortex and nucleus accumbens of subjects with opioid use disorder (OUD) [12, 20] as well as in preclinical models of OUD [20].

Preclinical studies of cocaine, alcohol or opioid use demonstrate that alteration of specialized ECM structures called perineuronal nets (PNN) represent a key feature underlying reward memory in SUDs [8, 9, 17, 21-24]. PNNs are ECM structures that envelop populations of fast-firing inhibitory neurons, stabilizing synapses on those neurons and restricting synaptic plasticity [16, 22, 25, 26]. During acquisition of drug memories, endogenous proteases including matrix metalloproteases (MMPs) degrade PNN components to allow for formation of new synapses associated with reward memories. [11, 27-30]. Chronic drug use resulting in prolonged re-activation of memory circuits results in enhancement of PNN components, stronger than at baseline, which stabilizes reward associated synapses [9, 23, 24, 31-33] and may contribute to context-induced relapse [11, 27-30]. Evidence that degradation of PNNs in the corticostriatal circuit significantly weakens drug reward memories provides further support for this hypothesis [10]. The hippocampus is at the center of neurocircuitry involved in reward memory processing [34]. Specifically, accumulating evidence suggests that hippocampal sector CA1 is involved in integrating dopamine reward signaling with

contextual memories and in regulating reward expectation and extinction [35-37]. Additionally, alterations of hippocampal PNNs can impact several neurotransmitter systems associated with reward processing. For example, PNN degradation alters firing rate of inhibitory parvalbumin (PVB) neurons [38], as well as NMDAR/AMPAR trafficking [39] and hippocampal dopamine transmission [40].

Despite this evidence, there is a lack of information regarding PNNs in the hippocampus of subjects with SUD, limiting the translatability of preclinical findings and the development of ECM-based therapies for context induced relapse. Furthermore, subjects with SUD often have comorbid substance use and a high degree of comorbidity with major depressive disorder (MDD) [41]. These features are challenging to capture in preclinical models, potentially limiting translatability. We used a cohort of human postmortem samples from subjects with SUD with or without comorbid MDD to test the hypothesis that numerical density of PNNs is increased in sector CA1 of the hippocampus of subjects with SUD, accompanied by altered expression of genes related to ECM degradation and biosynthesis, synaptic regulation, and PVB expression. This cohort includes retrospective clinical assessments, toxicology reports, history of substance use and medication history, allowing for testing of several of the features inherent in the population with SUD. Subjects with comorbid SUD and MDD, and subjects with MDD without SUD were included to examine the potential effects of comorbid MDD on ECM pathology in SUD. Furthermore, we used a collection of postmortem hippocampus samples from rhesus monkeys with or without chronic alcohol self-administration to examine the direct cause and effect on PNNs of the most common drug of abuse present across all our subjects with SUD.

MATERIALS AND METHODS

Postmortem brain samples

Human subjects for brightfield microscopy and RNA studies

Fresh frozen blocks containing the hippocampus from subjects with SUD (n=20), SUD and comorbid MDD (n=24), MDD (n=20), and psychiatrically normal controls (n=20) were provided by the UMMC Postmortem Brain Core (Table 1). Details are described in our previous report [42] and in the Supplemental Materials.

Psychiatric control subjects for immunofluorescence imaging

Fixed free-floating samples containing the hippocampus were obtained from the Harvard Brain Tissue Resource Center. Two psychiatrists determined the absence of DSM-IV diagnoses based on the review of a questionnaire filled out by legal next of kin and a review of all available medical records. Control cases had sufficient information from legally-defined next of kin and medical records to rule out major medical, neurologic, and psychiatric conditions. All brains underwent a complete neuropathological exam and cases with histopathological abnormalities were excluded from this study.

Rhesus macaque subjects

Fresh frozen hippocampus samples from adult male rhesus macaques (*Macaca mulatta*) with or without chronic alcohol administration were obtained from the Monkey Alcohol Tissue Research Resource (MATRR) Cohort 5 (Table 1). Details regarding these subjects are available at www.matrr.com and described in the Supplemental Materials.

Tissue collection and processing

Human postmortem samples for brightfield microscopy

Coronal serial sections (14 μm) were obtained from fresh frozen postmortem hippocampal blocks. Blocks were dissected and rapidly frozen in 2-methylbutane and on dry ice without fixation and

kept in dry ice before permanent storage at -80 °C. Blocks were sectioned using a Leica CM3050S cryostat.

Multiplex immunofluorescence control cohort

Tissue blocks containing the hippocampus were dissected from fresh brains and post-fixed in 0.1 M phosphate buffer (PB) containing 4% paraformaldehyde and 0.1 M sodium azide at 4◦C for 2 weeks, then stored in cryoprotectant solution at -20◦C (30% glycerol, 30% ethylene glycol, and 0.1% Na azide in 0.1 M PB), embedded in agar, and pre-sliced in 2 mm coronal slabs using an Antithetic Tissue Slicer (Stereological Research Lab., Aarhus, Denmark). Each slab was sectioned using a freezing microtome (American Optical 860, Buffalo, NY, United States). Sections were stored in cryoprotectant at –20◦C. Three 50 µm thick sections per subject were chosen for multiplex immunofluorescence labeling.

Histochemical/immunocytochemical labeling, imaging, and quantification procedures

Brightfield microscopy

Fresh-frozen, slide-mounted medial hippocampal cryosections from human subjects and rhesus macaque subjects (3-5 sections per subject) were post-fixed for 30 minutes in 4% paraformaldehyde, followed by 1 hour incubation in 2% bovine serum albumin (BSA), and overnight incubation in biotinylated *Wisteria floribunda agglutinin* (WFA) lectin (1:500, catalog #B-1355, Vector Labs). WFA binds to non-sulfated N-acetyl-D-galactosamine residues on the terminal ends of CSPGs [43]. The following day, tissue was incubated in streptavidin horseradish peroxidase (1:5000 µl, Zymed, San Francisco, CA) for four hours, followed by a 20-minute incubation in 3’3-diaminobenzidine with nickel sulfate hexahydrate and H_2O_2. Tissue was dehydrated through an ethanol and xylene series, followed by histological labeling with Methyl Green (catalog #H-3402, Vector Labs). Sections were coverslipped and coded for blinded quantitative analysis. All sections included in the study were processed simultaneously to avoid

procedural differences. WFA-labeled PNNs and glial cells were quantified using an Olympus BX61 microscope. Each anatomical subdivision of the hippocampus was traced for an area measurement using a 20X objective, and WFA-labeled elements were quantified on 40X magnification using Stereo-Investigator v11.

Immunofluorescence and Confocal imaging

Free-floating 50 µm thick sections containing the human hippocampus were carried through antigen retrieval in citric acid buffer (0.1 M citric acid, 0.2 M Na2HPO4) heated to 80 degrees °C for 30 minutes, incubated in 2% BSA for one hour. and incubated for two nights at 4 °C in biotinylated WFA lectin (catalog #B-1355, Vector Labs), PVB (catalog #P3088, Sigma-Aldrich), VAMP2 (catalog #10135-1-AP, ProteinTech), and SYN1 (catalog #20258-1-AP, ProteinTech) antibodies. Following primary antibody incubation, samples were incubated in alexa fluor streptavidin 488 (1:3000, cat# S11223, Invitrogen), goat anti-mouse 647 (1:300, cat#A28181), and goat anti-rabbit 555 (1:300; cat# A32732) for 4 hours, followed by incubation in Trueblack lipofuscin autofluorescence quencher (cat#23007, Biotum). Sections were mounted on gelatin coated glass slides and coverslipped with Dako fluorescent mounting media (cat#S3023, Agilent Technologies). A Zeiss LSM 880 confocal microscope interfaced with Zen imaging software (ZEN 2.3 SP1) was used to acquire images of PVB interneurons with WFA+ PNNs and VAMP2 or SYN1 labeling. Images were acquired with a z-step of 0.5 µm using a 63x oil immersion objective (numerical aperture 1.4 DIC M27; pixel size, 0.10 × .10 µm). Maximum intensity projections were acquired using Zen Blue (ZEN 2.6) software, compiling all images taken on the three-dimensional z-axis into a single, two-dimensional, multichannel image (Figure 2B and 2D).

Quantitative polymerase chain reaction

qPCR was conducted as described previously [42, 44] and in the Supplemental Materials. The primers used are listed in Supplemental Table 21.

Statistical Analysis

Numerical densities of microscopy measures were calculated as described in our previous studies [45] [46, 47]. The goal of our study was to test for differences in hippocampal CA1 stratum oriens PNN densities and hippocampal gene expression of ECM and synaptic markers between diagnosis groups. Analysis of WFA-glial densities was focused on the DG and CA4 areas where these cells are primarily distributed in the hippocampus in our current study and our previous report [45]. Diagnosis groups with comorbid SUD/MDD and MDD were included to test for potential effects of comorbid depression on findings in SUD. Exploratory analysis was conducted on microscopy measures of PNNs and WFA-glia on additional hippocampal sectors. Differences between groups relative to the main outcome measures were assessed for statistical significance using stepwise linear regression analysis of covariance (ANCOVA) using JMP Pro v16.1.0 (SAS Institute Inc., Cary, NC). Logarithmic transformation was applied to values when not normally distributed. Potential confounding variables (Table 1 and Supplementary Tables 5-20) were tested systematically for their effects on main outcome measures and included in the model if they significantly improved goodness-of-fit. Covariates found to significantly affect outcome measures are reported. Subjects with SUD, subjects with SUD/MDD, and subjects with MDD were first compared separately with psychiatrically-normal controls. Subsequently, the four groups were considered together to test for differences between diagnostic groups and Bonferroni correction applied for multiple comparisons.

RESULTS

Altered PNN and WFA-glia densities in subjects with SUD, MDD, and comorbid SUD/MDD

Numerical densities of PNNs were significantly increased in CA1 stratum oriens of subjects with SUD ($p < 0.007$; adjusted for significant effects of PMI and cocaine history). (Figure 1A-C). Further analysis of additional hippocampal sectors revealed increased numerical densities of PNNs in

CA2 stratum oriens ($p < 0.03$; adjusted for significant effects of age), CA2 stratum pyramidale ($p < 0.0001$; adjusted for significant effects of cocaine history), CA3 stratum oriens ($p <0.01$; adjusted for significant effects of cocaine history), and CA4 ($p < 0.007$; adjusted for significant effects of cocaine history) in subjects with SUD (Table S1). History of cocaine use, which was a significant covariate across hippocampal subregions, was associated with decreased PNNs in each of these regions. No significant differences were found in the dentate gyrus or the CA1 and CA3 stratum pyramidale layers. In subjects with MDD, we observed significantly decreased numerical densities of PNNs in CA1 stratum oriens ($p < 0.05$; adjusted for significant effects of sex and calcium channel blockers) and CA1 stratum pyramidale ($p < 0.02$), increased PNNs in CA4 ($p < 0.01$; adjusted for significant effects of anxiety disorder diagnoses), and no significant differences in other regions of the hippocampus. The duration of illness positively correlated with PNN density in CA1 stratum oriens across subjects with MDD (Supplemental Figure 1A). In subjects with comorbid SUD/MDD, we observed reduced numerical densities of PNNs in CA1 stratum pyramidale ($p < 0.02$; adjusted for significant effects of substance abuse history and duration of MDD), increased densities of PNNs in CA2 stratum pyramidale ($p < 0.01$; adjusted for significant effects of SSRIs in the toxicology report and ZT time). No significant differences were observed in the other hippocampal subregions. Table S1 contains information for each hippocampus subregion, including p-values, F-ratios, adjusted least squares means, standard error, and significant covariates.

We observed WFA-labeled glial cells in addition to PNN labeling. WFA-glia in our current study were identical to WFA-glia described our previous reports in the human medial temporal lobe where they were shown to co-express the astrocyte marker glial fibrillary acidic protein (GFAP) [46, 47]. WFA-glial cells were distributed primarily in the dentate gyrus and CA4 areas, with sparse expression in other hippocampal subregions (Figure 1E-F). In subjects with SUD, we observed significantly greater density of WFA-glia in the dentate gyrus ($p < 0.02$; adjusted for significant

effects of cocaine history), and significantly decreased density of WFA-glia in CA4 ($p < 0.02$; adjusted for significant effects of age, ZT time of death, and diagnosis–ZT interaction). No other hippocampal subregions displayed statistically significant differences in subjects with SUD. In subjects with MDD, we observed significantly increased densities of WFA-glia in the dentate gyrus ($p < 0.0001$), CA3 stratum pyramidale ($p < 0.0008$; adjusted for a significant effect of antidepressants in last month of life), CA2 stratum pyramidale ($p < 0.006$; adjusted for a significant effect of antidepressants in last month of life), and CA2 stratum oriens ($p < 0.02$). All other hippocampal subregions lacked differences in subjects with MDD. In subjects with comorbid SUD/MDD, we observed significantly decreased numerical densities of WFA-glia in the dentate gyrus ($p < 0.02$; adjusted for significant effects of alcohol in the toxicology report and calcium channel blockers), CA4 ($p < 0.02$; adjusted for a significant effect of alcohol in the toxicology report), CA3 stratum pyramidale ($p < 0.002$; adjusted for significant effects of alcohol in the toxicology report and race), CA2 stratum pyramidale ($p < 0.004$; adjusted for a significant effect of race), CA1 stratum pyramidale ($p < 0.02$; adjusted for significant effects of antipsychotics and alcohol in the toxicology report), and CA1 stratum oriens ($p < 0.02$; adjusted for a significant effect of race) when compared to psychiatric control subjects. Table S2 contains information for each hippocampus subregion. No differences in hippocampal area measurements were detected between control subjects and any of the diagnosis groups (Supplementary Table S4).

Gene expression of markers for cell populations associated with PNNs and WFA-glial cells

Parvalbumin. Neurons expressing parvalbumin (*Pvb*) mRNA represent the majority of neurons surrounded by PNNs in the hippocampus [45, 48, 49]. Subjects with SUD had significantly greater mRNA expression of *Pvb* compared to control subjects (Fig. 1D, Table S3; $p <0.007$; adjusted for a significant effect of cocaine history). Subjects in the SUD group with cocaine in the blood at death had significantly lower *Pvb* mRNA expression compared to subjects with SUD without cocaine in the blood at death (Supplemental Figure 1G). *Pvb* mRNA was also significantly greater

in subjects with comorbid SUD/MDD ($p < 0.008$), and subjects with MDD ($p < 0.005$) compared to control subjects (Fig. 1D, Table S3).

Glial fibrillary acidic protein. The astrocyte marker glial fibrillary acidic protein (Gfap), has been previously reported to co-localize with astrocytes labeled by WFA in the human brain [46, 50]. *Gfap* mRNA expression was significantly lower in the hippocampus of subjects with comorbid SUD/MDD ($p < 0.02$; adjusted for significant effects of SSRIs in last month of life which increases *Gfap*) (Fig. 1H, Table S3). No changes were detected in the SUD or MDD groups.

Altered expression of synaptic markers in the hippocampus of subjects with SUD

Synaptobrevin and Synapsin 1. Synaptobrevin (VAMP2) is an excitatory synaptic marker that contributes to the SNARE complex, allowing for fusion of vesicles to the cell membrane to facilitate neurotransmitter exocytosis and receptor trafficking [51, 52]. We examined VAMP2 as a step towards investigating altered synaptic regulation in the hippocampus of subjects with SUD as suggested by extensive literature indicating altered synaptic regulation by chronic exposure to substances of abuse (for review see [53]). We first tested whether VAMP2 protein is located on PVB neurons and in PNNs, We observed VAMP2 protein on PVB neurons ensheathed by PNNs, and enmeshed within the PNN (Figure 2B). In subjects with SUD, *Vamp2* mRNA was significantly increased ($p < 0.04$; adjusted for a significant effect of sleep quality). A significant increase in *Vamp2* mRNA expression was also observed in subjects with MDD ($p < 0.005$; with significant effects of age, ZT time, and sleep disturbance). No changes in *Vamp2* expression were detected in subjects with comorbid SUD/MDD. We conducted similar analysis for the inhibitory presynaptic marker, synapsin 1 (*Syn1*). We observed spatial overlap of SYN1 protein with PVB interneurons coated by PNNs, including SYN1 within PNNs (Figure 2D). In contrast to Vamp2, no significant differences were observed for Syn1 gene expression in any of the diagnostic groups (Figure 2).

Altered expression of ECM molecules in the hippocampus of subjects with SUD

Matrix metalloproteinase 9 (Mmp9) and Cathepsin S (Ctss). Significantly decreased mRNA expression of *Mmp9* was observed in subjects with SUD (Fig. 3A ; $p < 0.04$). Furthermore, *Ctss* mRNA was significantly decreased in subjects with SUD (Fig. 3B; $p < 0.03$; with significant effects of cocaine in the toxicology report) and increased in subjects with MDD ($p < 0.04$; adjusted for significant effects of alcohol use severity and ZT time). No significant changes were observed in subjects with comorbid SUD/MDD (Fig. 3A&B).

Aggrecan (Acan) and Chondroitin synthase 1 (Chsy1). In subjects with SUD/MDD, we observed significantly increased aggrecan (*Acan)* (Fig. 3C; $p < 0.03$), as well as chondroitin synthase 1 (*Chsy1)* mRNA (Fig. 3D; $p < 0.0001$; with significant effects of duration of AUD and tissue pH). In subjects with SUD, a significant increase in *Chsy1* expression was detected (Fig. 3D; $p < 0.04$; with a significant effect of tissue pH), and no significant difference was observed for *Acan (Fig. 3C)*. No changes were observed in subjects with MDD for either *Acan* or *Chsy1 (Fig. 3C&D)*.

Increased numerical densities of perineuronal nets in the hippocampus of monkeys with chronic alcohol self-administration

We observed a significant increase of PNNs in the combined hippocampal subfields in rhesus monkeys with chronic alcohol self-administration ($p < 0.03$). Similar increases were observed in CA1 stratum oriens (Fig. 4E; $p < 0.04$), CA3 stratum oriens (Fig. 4E; $p < 0.03$) and stratum pyramidale (Fig. 4E; $p < 0.02$), and CA2 stratum pyramidale (Fig. 4E; $p < 0.02$). We also detected significantly increased numerical densities of WFA-labeled glia in the dentate gyrus granule cell layer (Fig. 4F; $p < 0.04$). Finally, CA3 stratum pyramidale PNNs (Supplemental Fig 1C; $p < 0.01$) and dentate gyrus WFA-glia (Supplemental Fig. 1D; $p < 0.01$) positively correlated with average blood ethanol concentration.

DISCUSSION

Our data represent, to our knowledge, the first evidence for increased PNN densities in subjects with SUD and rhesus macaques with chronic alcohol self-administration. These findings link over a decade of evidence from preclinical models demonstrating increased PNNs in animals with chronic drug use [9, 17, 23, 24, 32, 54-56] with evidence in subjects with SUD. Together with the observed increased expression of the synaptic marker *Vamp2* and the CSPG synthesis molecule *Chsy1*, this suggests that enhanced PNN composition may aid in stabilizing contextual reward-associated synapses in the hippocampus of individuals with SUD. Furthermore, decreased expression of ECM proteolytic molecules indicates that changes in PNN densities are accompanied by decreased ECM remodeling in chronic SUD. Increased expression of parvalbumin, expressed by neurons that PNNs typically encapsulate, suggests increased feedforward inhibition of local excitatory pyramidal neurons by parvalbumin that increases coherence of drug-associated neuronal ensembles. In contrast, decreased densities of PNNs in subjects with MDD represent the first evidence for altered PNNs in the hippocampus of subjects with MDD. Taken together, our findings support the hypothesis that increased PNNs may stabilize contextual reward memories in subjects with SUD and thus may represent therapeutic targets for context-induced relapse. Furthermore, decreased densities of PNNs in subjects with MDD and lack of significant differences in subjects with comorbid SUD/MDD highlight the importance of considering comorbid conditions for both the neuropathology and treatment of SUD.

PNNs and ECM molecules in the Hippocampus of Subjects with Substance Use Disorder

SUDs are chronically relapsing disorders which rely heavily on memory salience (i.e., cue responsiveness). Our findings support an increasing number of preclinical studies for increased PNNs in SUD, suggesting that PNNs stabilize reward memories [8, 9, 16, 17, 22-24, 33]. Furthermore, PNNs are involved in a wide range of processes that can impact context induced relapse including stabilization of synapses, receptor trafficking, and regulation of interneuron activity [25, 26, 38, 39, 57-63].

Previous studies have implicated each of these processes in SUD. For example, chronic substance use has been shown to elicit downstream alteration of synapses and neurotransmitters including changes in dopamine 2 receptors (D2R) [64] as well as glutamatergic and GABAergic systems [65, 66]. PNNs contribute to synaptic homeostasis through the stabilization of synapses and PVB interneuron-mediated excitatory/inhibitory balance [67]. Thus, PNNs may stabilize synapses involved in drug reward processes that contribute to context induced relapse [18].

The association of PVB interneurons with PNNs has been demonstrated in several brain areas, including the hippocampus [45, 68-70]. Hippocampal PVB neurons are predominantly located in the stratum oriens layers of the CA regions. PVB neurons are involved in modulating glutamatergic neurons and hippocampal output to regions involved in reward processing [71, 72]. Increased PVB expression is positively correlated with PNN labeling [73] and removal of PNNs with chondroitinase ABC or antidepressants decreases PVB interneuron activity [74]. Increased PVB expression in SUD may induce feedforward inhibition of local excitatory neurons that enhances coherence of drug-specific neuronal ensembles [75]. Enhanced PNN composition on PVB neurons may also contribute to increased PVB expression and downstream consequences on excitatory/inhibitory balance which can result in altered activity of reward circuits involved in reward prediction and impulsivity [76, 77]. Importantly, *Pvb* expression was significantly decreased in subjects with cocaine in their toxicology reports (Supplementary Figure 1G), suggesting that cocaine temporarily blunts PVB expression to disinhibit excitatory neurons [55]. Furthermore, decreased ECM proteolytic gene expression (*Mmp9* and *Ctss*) in subjects with SUD is in line with increased PNN densities in these subjects, suggesting hypofunction of PNN proteolytic systems [78]. In our ANCOVA models, subjects with SUD who had cocaine in their toxicology reports had greater expression of *Ctss* (Supplementary Figure 1H). Speculatively, increased *Ctss* and decreased *Pvb* in subjects with cocaine in the toxicology report may indicate that cocaine temporally activates *Ctss* to temporarily degrade PNNs and decrease in *Pvb* expression.

There is extensive evidence demonstrating a central role of the hippocampus for episodic memory processing [79]. Furthermore, the hippocampus has bi-directional connections with the amygdala that contribute to assigning emotional valence to contextual memories, which is crucial in the long-term retention of drug memories [80]. Hippocampal connections with the ventral tegmental area (VTA) are involved in regulating memory salience and reward predictions. Hippocampal glutamatergic fibers from CA1 travel through the subiculum to basal forebrain structures, and synapse onto VTA neurons which feed back to the hippocampus to release dopamine [76, 77]. Thus, increased PNNs in the hippocampus of subjects with SUD can impact this system and contribute to several aspects of reward memory circuits.

Our studies represent first description of increased numerical densities of WFA-glial cells in individuals with SUD. Despite previous evidence that WFA-glia colocalize with the astrocytic marker GFAP [46, 47], we did not detect increased GFAP expression in subjects with SUD, suggesting that increases in WFA-glia do not reflect a broader astrogliosis process. Increased WFA-glia in the hippocampus may indicate impaired maturation of hippocampal cells in SUD, which has been previously implicated in patients with alcohol use disorder [81, 82].

We used a proximal specie, *Macaca mulatta*, with or without chronic alcohol use to test for specific effects of the most common drug in our cohort without the covariates inherent to cross-sectional human studies. Increased PNN densities and WFA-glia in rhesus monkeys with chronic alcohol use provides support for our findings in human subjects. Furthermore, the ability of chronic alcohol use alone to induce these changes is intriguing and represents the first evidence for increased PNNs in the hippocampus of non-human primates in response to any drug of abuse. The present findings also represent the first observation of WFA-labeled glia in the non-human primate brain; to this point, they have only been reported in human subjects [45, 46, 69]. These WFA-glial cell increases may represent enhanced CSPG synthesis by astrocytes or impaired maturation of oligodendrocyte progenitor cells [83]. Furthermore, increased densities of WFA-

labeled glia in the dentate gyrus of both humans with SUD and monkeys with chronic alcohol self-administration may be indicative of impaired adult neurogenesis in SUD [81, 82].

PNNs and ECM molecules in the Hippocampus of Subjects with Comorbid Substance Use Disorder and Major Depressive Disorder

Subjects with comorbid SUD and MDD represent a significant population of people with SUD and a bi-directional disorder where dysphoria can fuel the inclination to self-medicate. Alternatively, chronic drug use can contribute to mood disturbances [84]. Despite this relationship, co-occurrence of MDD and SUD is not typically examined in postmortem brain studies. Our results suggest MDD comorbidity is an important factor in studies of SUD. Inclusion of subjects with MDD may either mask or amplify changes present in each disorder. Most of our outcome measures displayed opposing directionality between subjects with SUD and MDD. For example, density of CA1 SO PNNs was significantly increased in SUD, decreased in MDD, and unaltered in subjects with comorbid SUD/MDD. In comparison, a comorbid diagnosis of MDD appeared to significantly amplify the existing increased expression of *Chsy1* observed in subjects with SUD (Figure 3D).

Increased mRNA expression of *Chsy1* in SUD and subjects with SUD/MDD may suggest that increased biosynthesis of CSPGs by chronic drug use is enhanced by processes underlying MDD. Expression of the CSPG aggrecan, a major PNN component [85], was increased in subjects with comorbid SUD/MDD. This may represent alterations in PNN composition that are not detected by standard WFA labeling.

PNNs and ECM molecules in the Hippocampus of Subjects with Major Depressive Disorder

A strength of our cohort was the ability to cross-examine the incidence of MDD comorbid with SUD as well as subjects with MDD only. Approximately one third of patients with MDD also experience SUD, and conversely a substantial proportion of individuals with SUD will experience MDD at some point during prognosis [41, 86]. This bi-directional comorbidity contributes to a

heightened risk of suicide and greater social and personal impairment [87]. While densities of PNNs were decreased in subjects with MDD (Fig. 1C), the duration of MDD positively correlated with densities of PNNs in CA1 stratum oriens (Supplementary Figure 1A). This is in line with preclinical evidence demonstrating that animals exposed to chronic social defeat display increased PNNs in the hippocampus [88]. Over time, increased PNNs may alter E/I balance contributing to decreased hippocampal sharp wave ripple events that negatively affect mood and memory [89, 90]. Increased expression of VAMP2 in subjects with MDD is in line with preclinical evidence for glucocorticoid-mediated calcium influx increases in hippocampal CA regions which perturbs plasticity, potentially resulting in poorer cognitive performance [91]. Increased VAMP2 is also in agreement with evidence indicating altered synaptic markers in MDD [92]. Decreases in PNNs may result in reduced stabilization of synapses and contribute to synaptic alterations, potentially resulting in memory impairment, memory generalization, and cognitive deficits observed in MDD [93]. An extensive number of studies implicate glial cell alterations in the pathology of depression (for review see [94]). In patients with SUD/MDD, we observed decreased expression of *Gfap*. A similar nonsignificant trend for decreased Gfap expression was observed in subjects with MDD. In our ANCOVA models, *Gfap* expression was significantly affected by history of SSRI exposure, which was positively associated with *Gfap* expression (Supplementary Figure 1B), suggesting that therapeutic effects of SSRIs may in part normalize *Gfap* levels, possibly reflecting glial progenitor cell maturation as suggested by previous studies [95, 96]. Our observed increase of *Ctss* gene expression may represent a heightened inflammatory state in the hippocampus of subjects with MDD, which has been extensively implicated in MDD [97, 98], including in the hippocampus in a cohort that largely overlaps with our cohort of subjects with MDD [99].

TECHNICAL CONSIDERATIONS

Several factors represent challenges in examining molecular pathology in the brain of subjects with SUD, including polysubstance use, comorbidity with MDD, and pharmacological treatments.

However, considering that this is representative of the real-world population of SUD it is important to examine the molecular pathology when these factors are present in the same subjects when considering development of therapeutic treatment strategies for this population. Our cohort consists of extensive information including retrospective clinical assessments, history of specific drugs of abuse and presence or absence of drugs of abuse and psychiatric medications in the blood at death from toxicology reports that can be accounted for using ANCOVA analyses, as conducted in our previous study using this same cohort [42]. Furthermore, the inclusion of samples from rhesus monkeys with chronic alcohol use provides a valuable cause and effect comparison for the most common drug of abuse in our human subjects. The development of additional collections of NHP brain samples containing subjects self-administering specific drugs of abuse alone or in combination would further aide in interpreting human postmortem brain studies and guiding strategies for novel treatment development. For our microscopy studies, use of WFA lectin provides a standard view of a specific population of PNNs, as it binds to non-sulfated N-acetyl-D-galactosamine [43]. There are other populations of PNNs that can be detected with alternative labeling methods which may surround complementary populations of neurons, such as excitatory neurons or somatostatin interneurons [83, 100]. Future studies with additional markers for PNN core proteins and sulfation motifs will provide insight into the specific components of PNNs in SUD. Lastly, measurements of mRNA by qPCR do not identify the cell-types responsible for synthesis or functional activity of any of the genes measured.

CONCLUSIONS

In summary, our findings represent the first evidence for increased numerical densities of PNNs in the hippocampus of human subjects with SUD. Increased densities of hippocampal PNNs, together with decreased expression of ECM proteolytic genes and altered synaptic markers supports preclinical studies that suggest that PNNs may stabilize reward memories. Thus, PNNs and ECM molecules may represent promising targets for addressing context induced

relapse in SUD. In comparison, subjects with MDD displayed generally opposite effects for many of the main outcome measures and subjects with SUD with a comorbid diagnosis of MDD suggesting that ECM changes in MDD oppose changes in SUD. These findings highlight the importance of considering comorbidities regarding SUD pathology and treatment strategies.

Funding: This work was funded by support from the National Institute of Mental Health (R01 MH125833 and R01 MH117460), the National Institute of Alcoholism and Alcohol Abuse (P60AA010760, R24AA019431, F31 AA030166 and R01 AA029023), National Institute of Health (P51OD011092) and the Postmortem Brain Core of the Center for Psychiatric Neuroscience, funded through an IDeA COBRE award from the National Institute of General Medical Sciences (P30 GM103328).

Acknowledgements: The authors deeply appreciate the invaluable contributions made by the families consenting to donate brain tissue and be interviewed. We also gratefully acknowledge the support of the staff of the Cuyahoga County Medical Examiner's Office, Cleveland, Ohio. We acknowledge the expert assistance of Drs. James C. Overholser, George Jurjus, Lisa C. Konick, and of Lesa Dieter in establishing the psychiatric diagnoses, acquiring written consent and in collecting the tissues. For some of the subjects, the services of Timothy M. De Jong in acquiring written consent and Lisa Larkin and Nicole Herbst in tissue collection are gratefully acknowledged.

Conflict of Interest Statement: The authors have no competing financial interests to disclose.

Data Availability Statement: The data and original contributions presented in this study are included in the manuscript or supplemental materials. Further inquiries can be directed to the corresponding author.

REFERENCES

1. Grant BF, Saha TD, Ruan WJ, Goldstein RB, Chou SP, Jung J *et al.* Epidemiology of DSM-5 Drug Use Disorder: Results From the National Epidemiologic Survey on Alcohol and Related Conditions-III. *JAMA Psychiatry* 2016; **73**(1)**:** 39-47.

2. SAMHSA. Key substance use and mental health indicators in the United States: Results from the 2017 National Survey on Drug Use and Health. In: Services USDoHaH (ed). www.samhsa.gov/data, 2018.

3. Zironi I, Burattini C, Aicardi G, Janak PH. Context is a trigger for relapse to alcohol. *Behav Brain Res* 2006; **167**(1)**:** 150-155.

4. Carter BL, Tiffany ST. Meta-analysis of cue-reactivity in addiction research. *Addiction* 1999; **94**(3)**:** 327-340.

5. Niaura RS, Rohsenow DJ, Binkoff JA, Monti PM, Pedraza M, Abrams DB. Relevance of cue reactivity to understanding alcohol and smoking relapse. *J Abnorm Psychol* 1988; **97**(2)**:** 133-152.

6. Weiss F. Neurobiology of craving, conditioned reward and relapse. *Curr Opin Pharmacol* 2005; **5**(1)**:** 9-19.

7. Janak PH, Chaudhri N. The Potent Effect of Environmental Context on Relapse to Alcohol-Seeking After Extinction. *Open Addict J* 2010; **3:** 76-87.

8. Xue YX, Xue LF, Liu JF, He J, Deng JH, Sun SC *et al.* Depletion of perineuronal nets in the amygdala to enhance the erasure of drug memories. *J Neurosci* 2014; **34**(19)**:** 6647-6658.

9. Slaker M, Churchill L, Todd RP, Blacktop JM, Zuloaga DG, Raber J *et al.* Removal of perineuronal nets in the medial prefrontal cortex impairs the acquisition and reconsolidation of a cocaine-induced conditioned place preference memory. *J Neurosci* 2015; **35**(10)**:** 4190-4202.

10. Brown TE, Forquer MR, Cocking DL, Jansen HT, Harding JW, Sorg BA. Role of matrix metalloproteinases in the acquisition and reconsolidation of cocaine-induced conditioned place preference. *Learn Mem* 2007; **14**(3)**:** 214-223.

11. Smith AW, Nealey KA, Wright JW, Walker BM. Plasticity associated with escalated operant ethanol self-administration during acute withdrawal in ethanol-dependent rats requires intact matrix metalloproteinase systems. *Neurobiol Learn Mem* 2011; **96**(2)**:** 199-206.

12. Seney ML, Kim SM, Glausier JR, Hildebrand MA, Xue X, Zong W *et al.* Transcriptional Alterations in Dorsolateral Prefrontal Cortex and Nucleus Accumbens Implicate Neuroinflammation and Synaptic Remodeling in Opioid Use Disorder. *Biol Psychiatry* 2021; **90**(8)**:** 550-562.

13. Browne CJ, Futamura R, Minier-Toribio A, Hicks EM, Ramakrishnan A, Martínez-Rivera F *et al.* Transcriptional signatures of heroin intake and seeking throughout the brain reward circuit. *bioRxiv* 2023**:** 2023.2001.2011.523688.

14. Chioma VC, Kruyer A, Bobadilla AC, Angelis A, Ellison Z, Hodebourg R *et al.* Heroin Seeking and Extinction From Seeking Activate Matrix Metalloproteinases at Synapses on Distinct Subpopulations of Accumbens Cells. *Biol Psychiatry* 2021; **89**(10)**:** 947-958.

15. Smith AC, Scofield MD, Kalivas PW. The tetrapartite synapse: Extracellular matrix remodeling contributes to corticoaccumbens plasticity underlying drug addiction. *Brain Res* 2015; **1628**(Pt A)**:** 29-39.

16. Slaker M, Blacktop JM, Sorg BA. Caught in the Net: Perineuronal Nets and Addiction. *Neural Plast* 2016; **2016:** 7538208.

17. Roura-Martinez D, Diaz-Bejarano P, Ucha M, Paiva RR, Ambrosio E, Higuera-Matas A. Comparative analysis of the modulation of perineuronal nets in the prefrontal cortex of rats during protracted withdrawal from cocaine, heroin and sucrose self-administration. *Neuropharmacology* 2020; **180:** 108290.

18. Valeri J, Gisabella B, Pantazopoulos H. Dynamic regulation of the extracellular matrix in reward memory processes: a question of time. *Frontiers in cellular neuroscience* 2023; **17:** 1208974.

19. Ray MH, Williams BR, Kuppe MK, Bryant CD, Logan RW. A Glitch in the Matrix: The Role of Extracellular Matrix Remodeling in Opioid Use Disorder. *Front Integr Neurosci* 2022; **16:** 899637.

20. Browne CJ, Futamura R, Minier-Toribio A, Hicks EM, Ramakrishnan A, Martinez-Rivera FJ *et al.* Transcriptional signatures of heroin intake and relapse throughout the brain reward circuitry in male mice. *Sci Adv* 2023; **9**(23)**:** eadg8558.

21. Vazquez-Sanroman DB, Monje RD, Bardo MT. Nicotine self-administration remodels perineuronal nets in ventral tegmental area and orbitofrontal cortex in adult male rats. *Addict Biol* 2017; **22**(6)**:** 1743-1755.

22. Fawcett JW, Fyhn M, Jendelova P, Kwok JCF, Ruzicka J, Sorg BA. The extracellular matrix and perineuronal nets in memory. *Mol Psychiatry* 2022; **27**(8)**:** 3192-3203.

23. Lasek AW, Chen H, Chen WY. Releasing Addiction Memories Trapped in Perineuronal Nets. *Trends Genet* 2018; **34**(3)**:** 197-208.

24. Chen H, He D, Lasek AW. Repeated Binge Drinking Increases Perineuronal Nets in the Insular Cortex. *Alcohol Clin Exp Res* 2015; **39**(10)**:** 1930-1938.

25. Gogolla N, Caroni P, Luthi A, Herry C. Perineuronal nets protect fear memories from erasure. *Science* 2009; **325**(5945)**:** 1258-1261.

26. Pizzorusso T, Medini P, Berardi N, Chierzi S, Fawcett JW, Maffei L. Reactivation of ocular dominance plasticity in the adult visual cortex. *Science* 2002; **298**(5596)**:** 1248-1251.

27. Wright JW, Masino AJ, Reichert JR, Turner GD, Meighan SE, Meighan PC *et al.* Ethanol-induced impairment of spatial memory and brain matrix metalloproteinases. *Brain Res* 2003; **963**(1-2)**:** 252-261.

28. Natarajan R, Harding JW, Wright JW. A role for matrix metalloproteinases in nicotine-induced conditioned place preference and relapse in adolescent female rats. *J Exp Neurosci* 2013; **7:** 1-14.

29. Smith AC, Kupchik YM, Scofield MD, Gipson CD, Wiggins A, Thomas CA *et al.* Synaptic plasticity mediating cocaine relapse requires matrix metalloproteinases. *Nat Neurosci* 2014; **17**(12)**:** 1655-1657.

30. Stefaniuk M, Beroun A, Lebitko T, Markina O, Leski S, Meyza K *et al.* Matrix Metalloproteinase-9 and Synaptic Plasticity in the Central Amygdala in Control of Alcohol-Seeking Behavior. *Biol Psychiatry* 2017; **81**(11)**:** 907-917.

31. Van den Oever MC, Lubbers BR, Goriounova NA, Li KW, Van der Schors RC, Loos M *et al.* Extracellular matrix plasticity and GABAergic inhibition of prefrontal cortex pyramidal cells facilitates relapse to heroin seeking. *Neuropsychopharmacology* 2010; **35**(10)**:** 2120-2133.

32. Slaker ML, Jorgensen ET, Hegarty DM, Liu X, Kong Y, Zhang F *et al.* Cocaine Exposure Modulates Perineuronal Nets and Synaptic Excitability of Fast-Spiking Interneurons in the Medial Prefrontal Cortex. *eNeuro* 2018; **5**(5).

33. Lasek AW. Effects of Ethanol on Brain Extracellular Matrix: Implications for Alcohol Use Disorder. *Alcohol Clin Exp Res* 2016; **40**(10)**:** 2030-2042.

34. Goode TD, Maren S. Common neurocircuitry mediating drug and fear relapse in preclinical models. *Psychopharmacology (Berl)* 2019; **236**(1)**:** 415-437.

35. Goldsmith SK, Joyce JN. Dopamine D2 receptor expression in hippocampus and parahippocampal cortex of rat, cat, and human in relation to tyrosine hydroxylase-immunoreactive fibers. *Hippocampus* 1994; **4**(3)**:** 354-373.

36. Galvez-Marquez DK, Salgado-Menez M, Moreno-Castilla P, Rodriguez-Duran L, Escobar ML, Tecuapetla F *et al.* Spatial contextual recognition memory updating is modulated by dopamine release in the dorsal hippocampus from the locus coeruleus. *Proc Natl Acad Sci U S A* 2022; **119**(49)**:** e2208254119.

37. Krishnan S, Heer C, Cherian C, Sheffield MEJ. Reward expectation extinction restructures and degrades CA1 spatial maps through loss of a dopaminergic reward proximity signal. *Nature communications* 2022; **13**(1)**:** 6662.

38. Wingert JC, Sorg BA. Impact of Perineuronal Nets on Electrophysiology of Parvalbumin Interneurons, Principal Neurons, and Brain Oscillations: A Review. *Front Synaptic Neurosci* 2021; **13:** 673210.

39. Frischknecht R, Heine M, Perrais D, Seidenbecher CI, Choquet D, Gundelfinger ED. Brain extracellular matrix affects AMPA receptor lateral mobility and short-term synaptic plasticity. *Nat Neurosci* 2009; **12**(7)**:** 897-904.

40. Shah A, Lodge DJ. A loss of hippocampal perineuronal nets produces deficits in dopamine system function: relevance to the positive symptoms of schizophrenia. *Transl Psychiatry* 2013; **3**(1)**:** e215.

41. Mueller TI, Lavori PW, Keller MB, Swartz A, Warshaw M, Hasin D *et al.* Prognostic effect of the variable course of alcoholism on the 10-year course of depression. *Am J Psychiatry* 1994; **151**(5)**:** 701-706.

42. Valeri J, O'Donovan SM, Wang W, Sinclair D, Bollavarapu R, Gisabella B *et al.* Altered expression of somatostatin signaling molecules and clock genes in the hippocampus of subjects with substance use disorder. *Front Neurosci* 2022; **16:** 903941.

43. Nadanaka S, Miyata S, Yaqiang B, Tamura JI, Habuchi O, Kitagawa H. Reconsideration of the Semaphorin-3A Binding Motif Found in Chondroitin Sulfate Using Galnac4s-6st-Knockout Mice. *Biomolecules* 2020; **10**(11).

44. O'Donovan SM, Sullivan C, Koene R, Devine E, Hasselfeld K, Moody CL *et al.* Cell-subtype-specific changes in adenosine pathways in schizophrenia. *Neuropsychopharmacology* 2018; **43**(8)**:** 1667-1674.

45. Pantazopoulos H, Sawyer C, Heckers S, Berretta S, Markota M. Chondroitin Sulfate Proteoglycan Abnormalities in the Hippocampus of Subjects with Schizophrenia. *Neuropsychopharmacology* 2014; **39:** S298-S299.

46. Pantazopoulos H, Murray EA, Berretta S. Total number, distribution, and phenotype of cells expressing chondroitin sulfate proteoglycans in the normal human amygdala. *Brain Res* 2008; **1207:** 84-95.

47. Pantazopoulos H, Woo TU, Lim MP, Lange N, Berretta S. Extracellular matrix-glial abnormalities in the amygdala and entorhinal cortex of subjects diagnosed with schizophrenia. *Arch Gen Psychiatry* 2010; **67**(2)**:** 155-166.

48. Yamada J, Jinno S. Spatio-temporal differences in perineuronal net expression in the mouse hippocampus, with reference to parvalbumin. *Neuroscience* 2013; **253:** 368-379.

49. Rogers SL, Rankin-Gee E, Risbud RM, Porter BE, Marsh ED. Normal Development of the Perineuronal Net in Humans; In Patients with and without Epilepsy. *Neuroscience* 2018; **384:** 350-360.

50. Pantazopoulos H, Woo TU, Lim MP, Lange N, Berretta S. Extracellular matrix-glial abnormalities in the amygdala and entorhinal cortex of subjects diagnosed with schizophrenia. *Archives of general psychiatry* 2010; **67**(2)**:** 155-166.

51. Yan C, Jiang J, Yang Y, Geng X, Dong W. The function of VAMP2 in mediating membrane fusion: An overview. *Frontiers in Molecular Neuroscience* 2022; **15**.

52. Torres VI, Vallejo D, Inestrosa NC. Emerging Synaptic Molecules as Candidates in the Etiology of Neurological Disorders. *Neural Plast* 2017; **2017:** 8081758.

53. Neuhofer D, Kalivas P. Metaplasticity at the addicted tetrapartite synapse: A common denominator of drug induced adaptations and potential treatment target for addiction. *Neurobiology of Learning and Memory* 2018; **154:** 97-111.

54. Gonzalez AE, Jorgensen ET, Ramos JD, Harkness JH, Aadland JA, Brown TE *et al.* Impact of Perineuronal Net Removal in the Rat Medial Prefrontal Cortex on Parvalbumin Interneurons After Reinstatement of Cocaine Conditioned Place Preference. *Front Cell Neurosci* 2022; **16:** 932391.

55. Jorgensen ET, Gonzalez AE, Harkness JH, Hegarty DM, Thakar A, Burchi DJ *et al.* Cocaine memory reactivation induces functional adaptations within parvalbumin interneurons in the rat medial prefrontal cortex. *Addict Biol* 2021; **26**(3)**:** e12947.

56. Blacktop JM, Sorg BA. Perineuronal nets in the lateral hypothalamus area regulate cue-induced reinstatement of cocaine-seeking behavior. *Neuropsychopharmacology* 2019; **44**(5)**:** 850-858.

57. Kalb RG, Hockfield S. Molecular evidence for early activity-dependent development of hamster motor neurons. *J Neurosci* 1988; **8**(7)**:** 2350-2360.

58. Sugiyama S, Di Nardo AA, Aizawa S, Matsuo I, Volovitch M, Prochiantz A *et al.* Experience-dependent transfer of Otx2 homeoprotein into the visual cortex activates postnatal plasticity. *Cell* 2008; **134**(3)**:** 508-520.

59. Frischknecht R, Gundelfinger ED. The brain's extracellular matrix and its role in synaptic plasticity. *Adv Exp Med Biol* 2012; **970:** 153-171.

60. Dityatev A, Schachner M, Sonderegger P. The dual role of the extracellular matrix in synaptic plasticity and homeostasis. *Nat Rev Neurosci* 2010; **11**(11)**:** 735-746.

61. Gundelfinger ED, Frischknecht R, Choquet D, Heine M. Converting juvenile into adult plasticity: a role for the brain's extracellular matrix. *Eur J Neurosci* 2010; **31**(12)**:** 2156-2165.

62. Cabungcal JH, Steullet P, Morishita H, Kraftsik R, Cuenod M, Hensch TK *et al.* Perineuronal nets protect fast-spiking interneurons against oxidative stress. *Proc Natl Acad Sci U S A* 2013; **110**(22)**:** 9130-9135.

63. Morawski M, Bruckner MK, Riederer P, Bruckner G, Arendt T. Perineuronal nets potentially protect against oxidative stress. *Exp Neurol* 2004; **188**(2)**:** 309-315.

64. Trifilieff P, Martinez D. Imaging addiction: D2 receptors and dopamine signaling in the striatum as biomarkers for impulsivity. *Neuropharmacology* 2014; **76 Pt B**(0 0)**:** 498-509.

65. Li JN, Liu XL, Li L. Prefrontal GABA and glutamate levels correlate with impulsivity and cognitive function of prescription opioid addicts: A (1) H-magnetic resonance spectroscopy study. *Psychiatry Clin Neurosci* 2020; **74**(1)**:** 77-83.

66. D'Souza MS, Markou A. The "stop" and "go" of nicotine dependence: role of GABA and glutamate. *Cold Spring Harb Perspect Med* 2013; **3**(6).

67. Balmer TS. Perineuronal Nets Enhance the Excitability of Fast-Spiking Neurons. *eNeuro* 2016; **3**(4).

68. Steullet P, Cabungcal JH, Bukhari SA, Ardelt MI, Pantazopoulos H, Hamati F *et al.* The thalamic reticular nucleus in schizophrenia and bipolar disorder: role of parvalbumin-expressing neuron networks and oxidative stress. *Mol Psychiatry* 2017.

69. Pantazopoulos H, Woo T-UW, Lim MP, Lange N, Berretta S. Extracellular Matrix-Glial Abnormalities in the Amygdala and Entorhinal Cortex of Subjects Diagnosed With Schizophrenia. *Arch Gen Psychiatry* 2010; **67**(2)**:** 155-166.

70. Pantazopoulos H, Lange N, Hassinger L, Berretta S. Subpopulations of neurons expressing parvalbumin in the human amygdala. *The Journal of comparative neurology* 2006; **496**(5)**:** 706-722.

71. Espinoza C, Guzman SJ, Zhang X, Jonas P. Parvalbumin+ interneurons obey unique connectivity rules and establish a powerful lateral-inhibition microcircuit in dentate gyrus. *Nature Communications* 2018; **9**(1)**:** 4605.

72. Udakis M, Pedrosa V, Chamberlain SEL, Clopath C, Mellor JR. Interneuron-specific plasticity at parvalbumin and somatostatin inhibitory synapses onto CA1 pyramidal neurons shapes hippocampal output. *Nature Communications* 2020; **11**(1)**:** 4395.

73. Yamada J, Ohgomori T, Jinno S. Perineuronal nets affect parvalbumin expression in GABAergic neurons of the mouse hippocampus. *Eur J Neurosci* 2015; **41**(3)**:** 368-378.

74. Lesnikova A, Casarotto PC, Fred SM, Voipio M, Winkel F, Steinzeig A *et al.* Chondroitinase and Antidepressants Promote Plasticity by Releasing TRKB from Dephosphorylating Control of PTPσ in Parvalbumin Neurons. *J Neurosci* 2021; **41**(5)**:** 972-980.

75. Brown TE, Sorg BA. Net gain and loss: influence of natural rewards and drugs of abuse on perineuronal nets. *Neuropsychopharmacology* 2023; **48**(1)**:** 3-20.

76. Huang YY, Kandel ER. D1/D5 receptor agonists induce a protein synthesis-dependent late potentiation in the CA1 region of the hippocampus. *Proc Natl Acad Sci U S A* 1995; **92**(7)**:** 2446-2450.

77. Gasbarri A, Packard MG, Campana E, Pacitti C. Anterograde and retrograde tracing of projections from the ventral tegmental area to the hippocampal formation in the rat. *Brain Res Bull* 1994; **33**(4)**:** 445-452.

78. Samochowiec A, Grzywacz A, Kaczmarek L, Bienkowski P, Samochowiec J, Mierzejewski P *et al.* Functional polymorphism of matrix metalloproteinase-9 (MMP-9) gene in alcohol dependence: family and case control study. *Brain Res* 2010; **1327:** 103-106.

79. Eichenbaum H. Prefrontal–hippocampal interactions in episodic memory. *Nature Reviews Neuroscience* 2017; **18**(9)**:** 547-558.

80. Goodman J, Packard MG. Memory Systems and the Addicted Brain. *Frontiers in Psychiatry* 2016; **7**.

81. Murano T, Koshimizu H, Hagihara H, Miyakawa T. Transcriptomic immaturity of the hippocampus and prefrontal cortex in patients with alcoholism. *Sci Rep* 2017; **7:** 44531.

82. Miguel-Hidalgo JJ. Astroglia in the Vulnerability and Maintenance of Alcohol Use Disorders. *Adv Neurobiol* 2021; **26:** 255-279.

83. Pantazopoulos H, Markota M, Jaquet F, Ghosh D, Wallin A, Santos A *et al.* Aggrecan and chondroitin-6-sulfate abnormalities in schizophrenia and bipolar disorder: a postmortem study on the amygdala. *Translational Psychiatry* 2015; **5**(1)**:** e496-e496.

84. Markou A, Kosten TR, Koob GF. Neurobiological similarities in depression and drug dependence: a self-medication hypothesis. *Neuropsychopharmacology* 1998; **18**(3)**:** 135-174.

85. Roughley PJ, Mort JS. The role of aggrecan in normal and osteoarthritic cartilage. *Journal of Experimental Orthopaedics* 2014; **1**(1)**:** 8.

86. Gilman SE, Abraham HD. A longitudinal study of the order of onset of alcohol dependence and major depression. *Drug Alcohol Depend* 2001; **63**(3)**:** 277-286.

87. Young MA, Fogg LF, Scheftner WA, Fawcett JA. Interactions of risk factors in predicting suicide. *Am J Psychiatry* 1994; **151**(3)**:** 434-435.

88. Riga D, Kramvis I, Koskinen MK, van Bokhoven P, van der Harst JE, Heistek TS *et al.* Hippocampal extracellular matrix alterations contribute to cognitive impairment associated with a chronic depressive-like state in rats. *Sci Transl Med* 2017; **9**(421).

89. Blanco I, Conant K. Extracellular matrix remodeling with stress and depression: Studies in human, rodent and zebrafish models. *Eur J Neurosci* 2021; **53**(12)**:** 3879-3888.

90. Sun ZY, Bozzelli PL, Caccavano A, Allen M, Balmuth J, Vicini S *et al.* Disruption of perineuronal nets increases the frequency of sharp wave ripple events. *Hippocampus* 2018; **28**(1)**:** 42-52.

91. Karst H, Joëls M. Corticosterone Slowly Enhances Miniature Excitatory Postsynaptic Current Amplitude in Mice CA1 Hippocampal Cells. *Journal of Neurophysiology* 2005; **94**(5)**:** 3479-3486.

92. Duric V, Banasr M, Stockmeier CA, Simen AA, Newton SS, Overholser JC *et al.* Altered expression of synapse and glutamate related genes in post-mortem hippocampus of depressed subjects. *Int J Neuropsychopharmacol* 2013; **16**(1)**:** 69-82.

93. Perini G, Cotta Ramusino M, Sinforiani E, Bernini S, Petrachi R, Costa A. Cognitive impairment in depression: recent advances and novel treatments. *Neuropsychiatr Dis Treat* 2019; **15:** 1249-1258.

94. Miguel-Hidalgo JJ. Astrocytes as Context for the Involvement of Myelin and Nodes of Ranvier in the Pathophysiology of Depression and Stress-Related Disorders. *J Psychiatr Brain Sci* 2023; **8**.

95. Boldrini M, Underwood MD, Hen R, Rosoklija GB, Dwork AJ, John Mann J *et al.* Antidepressants increase neural progenitor cells in the human hippocampus. *Neuropsychopharmacology* 2009; **34**(11)**:** 2376-2389.

96. Boldrini M, Hen R, Underwood MD, Rosoklija GB, Dwork AJ, Mann JJ *et al.* Hippocampal angiogenesis and progenitor cell proliferation are increased with antidepressant use in major depression. *Biol Psychiatry* 2012; **72**(7)**:** 562-571.

97. Kohler-Forsberg O, C NL, Hjorthoj C, Nordentoft M, Mors O, Benros ME. Efficacy of anti-inflammatory treatment on major depressive disorder or depressive symptoms: meta-analysis of clinical trials. *Acta psychiatrica Scandinavica* 2019; **139**(5)**:** 404-419.

98. Fries GR, Saldana VA, Finnstein J, Rein T. Molecular pathways of major depressive disorder converge on the synapse. *Mol Psychiatry* 2023; **28**(1)**:** 284-297.

99. Mahajan GJ, Vallender EJ, Garrett MR, Challagundla L, Overholser JC, Jurjus G *et al.* Altered neuro-inflammatory gene expression in hippocampus in major depressive disorder. *Prog Neuropsychopharmacol Biol Psychiatry* 2018; **82:** 177-186.

100. Scarlett JM, Hu SJ, Alonge KM. The "Loss" of Perineuronal Nets in Alzheimer's Disease: Missing or Hiding in Plain Sight? *Front Integr Neurosci* 2022; **16:** 896400.

	SUD *n=20*	**SUD/MDD** *n=24*	**MDD** *n=20*	**Control** *n=20*
Age, Years	34.8±9.0	43.9±11.1	47±11.4	43.2±11.42
Sex				
Male	17	16	14	13
Female	3	8	6	7
Race				
White	13	20	17	11
Black	7	4	3	9
Brain pH	6.57±0.23	6.54±0.27	6.5±0.32	6.5±0.25
PMI, Hours	18.58±8.5	20.2±7.6	23.7±5.9	21.2±6.8

Rhesus macaque subjects		
	Alcohol drinkers *n*=7	**Control** *n*=5
Age, Years	7.20±0.04	6.90±0.49
Sex	Male (n=7)	Male (n=5)
BAC, mg pct	101.46±12.76	*NA*

Table 1. *Basic cohort demographic information for both human and rhesus macaque subjects.* Abbreviations: SUD, substance use disorder; MDD, major depressive disorder; PMI, postmortem interval, BAC, blood alcohol concentration, 12-month average. Values represent mean +/- standard error.

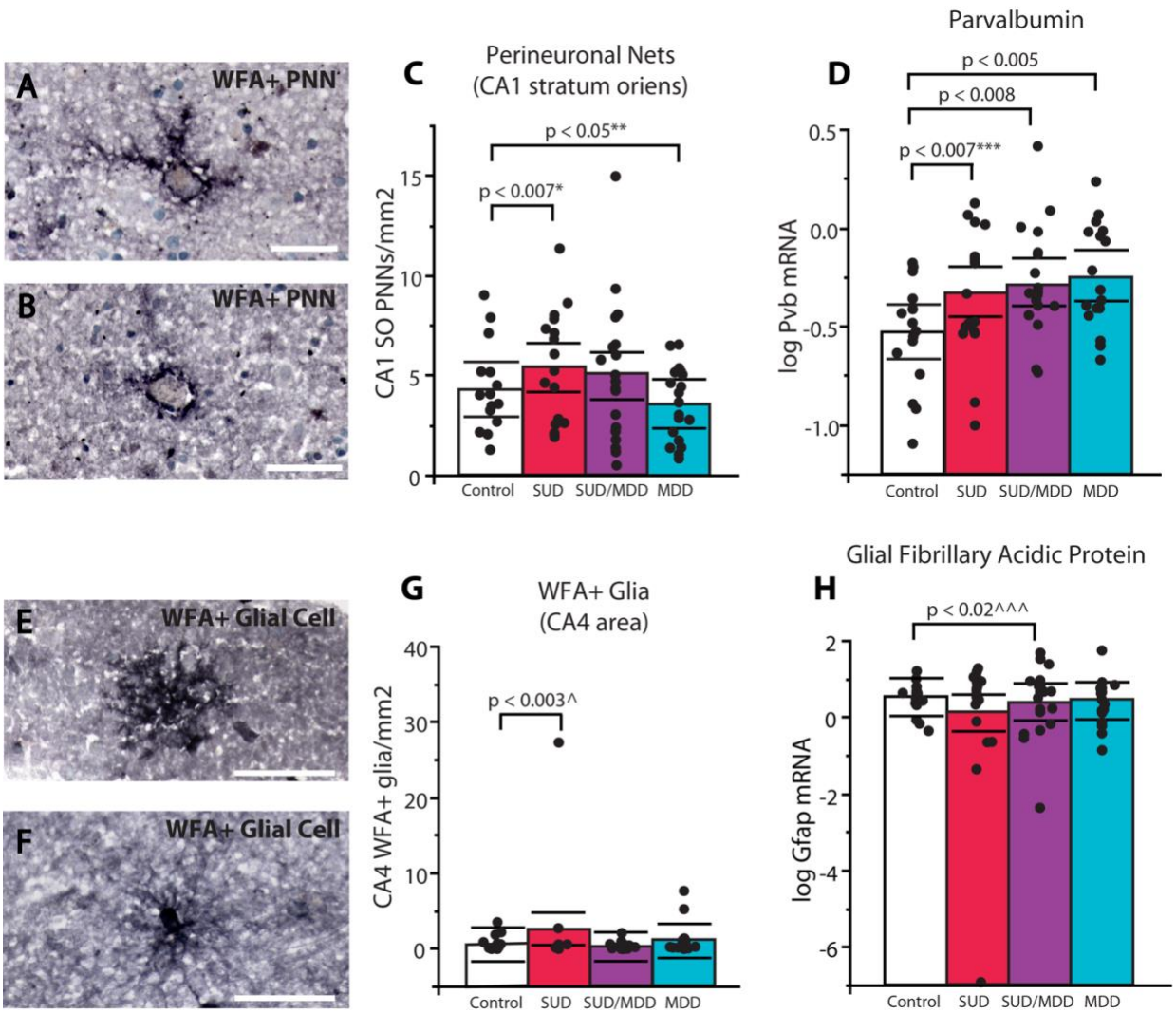

Figure 1. *Altered PNNs in SUD and MDD.* (A and B) Representative photomicrographs of PNNs labeled by *Wisteria floribunda agglutinin* lectin, scalebars = 100 µm. (C) Diagnostic group comparisons of PNN densities in CA1 stratum oriens. Subjects with SUD had significantly increased densities of PNNs ($p < 0.007$; adjusted for significant effects of cocaine history and PMI) whereas subjects with MDD displayed significantly reduced PNN densities ($p < 0.05$; adjusted for significant effects of sex and calcium channel blockers). No significant effects were found in the comorbid SUD and MDD group. (D) Diagnostic group comparisons of hippocampal *PVB* mRNA expression, with a gradient increase in SUD ($p < 0.007$; adjusted for significant effects of cocaine in the toxicology report), MDD/SUD ($p < 0.008$; adjusted for significant effects of MDD duration), and MDD ($p < 0.005$). (E and F) Representative photomicrographs of WFA-labeled CSPG glial cell morphology, scalebars = 100 µm. (G) Numerical density measurements of WFA-labeled glial cells in subjects with SUD, MDD, and comorbid SUD and MDD. (H) Gene expression of *Gfap* was significantly decreased in subjects with comorbid SUD and MDD ($p < 0.02$; adjusted for significant effects of antidepressant history), but unaffected in either disorder in isolation. Error bars are mean ± SEM.

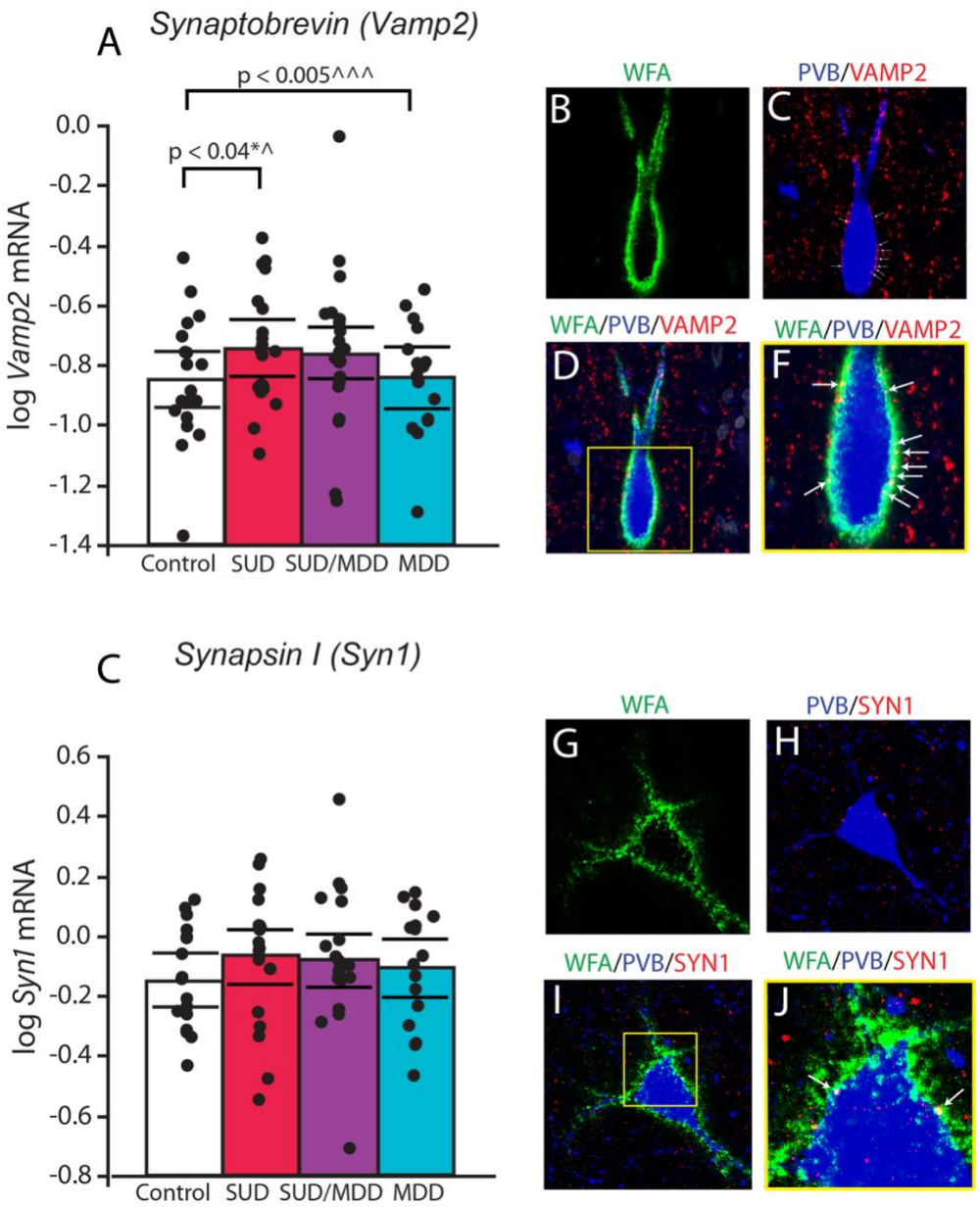

Figure 2. Gene expression of the *excitatory synaptic marker VAMP2 is altered in SUD and MDD.* (A) mRNA expression of the synaptic vesicle marker *Vamp2* is increased in both SUD and MDD, but not in the comorbid condition. (B-E) Multiplex immunofluorescent imaging of VAMP2 immunoreactive puncta within a PNN and on the surface of a PVB interneuron . (B) WFA-labeled PNN (green), (C) PVB interneuron (blue) and VAMP2 synaptic puncta (red) and spatial overlap (yellow) (arrows indicate overlap). (D) Composite z-projection of WFA, PVB, and VAMP2. (E) Zoomed inset of 1D, with arrows denoting spatial overlap of VAMP2 with WFA (yellow puncta). (F) There were no significant changes in transcription of the synaptic marker *Syn1* in any of the diagnostic groups. (G-J) Multiplex immunofluorescent imaging depicting SYN1 labeling within a PNN surrounding a PVB interneuron. (G) WFA-labeled PNN (green), (H) PVB neuron (blue) and SYN1 (red), (I) composite z-projection of all three channels. (J) Zoomed inset depicts spatial overlap with of SYN1 puncta with WFA labeling (arrows to yellow puncta). All scalebars are 10 µm. Error bars are mean ± SEM.

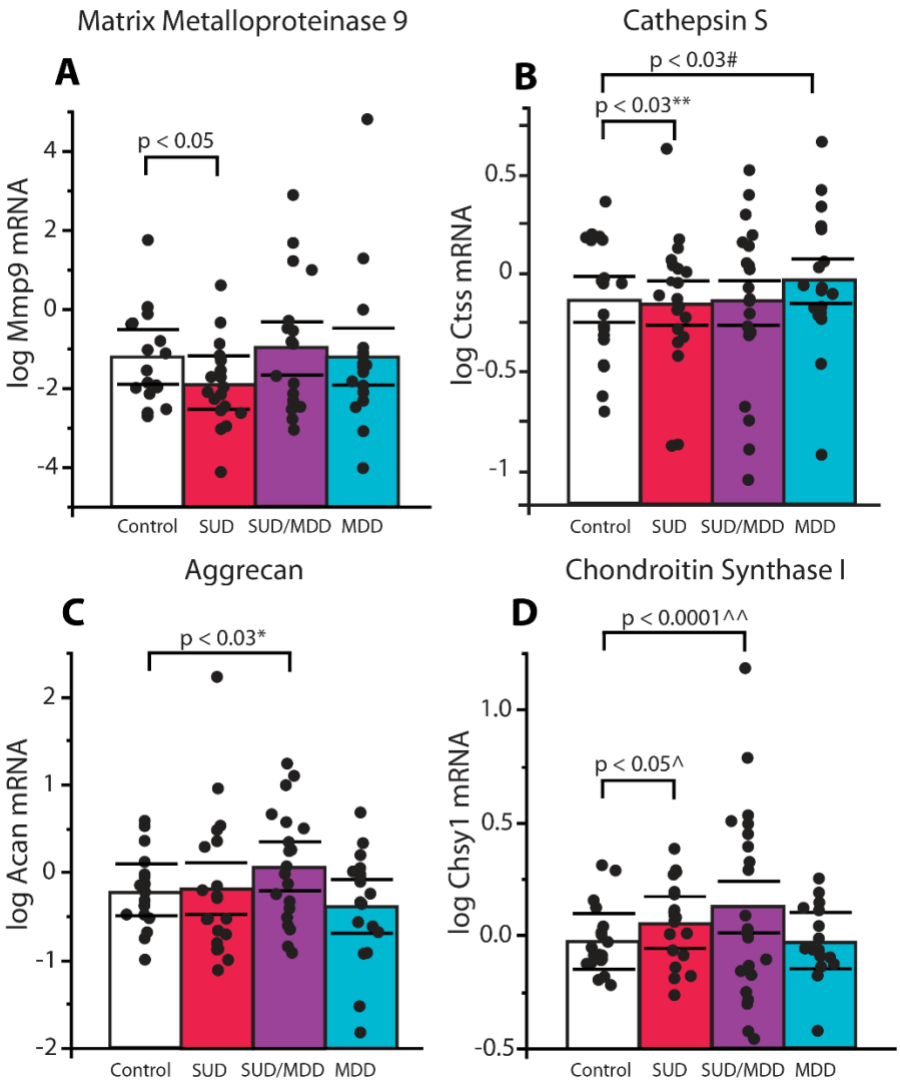

Figure 3. *Gene expression of ECM biosynthetic and regulatory molecules in SUD and MDD.* (A) Gene expression of the ECM proteolytic molecule *Mmp9* was significantly decreased in subjects with SUD compared to controls ($p < 0.05$), but no significant differences were detected in the other two diagnostic groups. (B) Analysis of covariance uncovered significantly decreased mRNA levels of cathepsin S in subjects with SUD ($p < 0.03$; adjusted for significant effects of cocaine in the toxicology report). Subjects with MDD had significantly increased expression of cathepsin S compared to controls ($p < 0.03$; adjusted for significant effects of alcohol history and ZT time of death). (C) Gene expression of the CSPG aggrecan was significantly increased in subjects with comorbid SUD and MDD ($p < 0.03$) but was unaffected in either condition separately. (D) Gene expression of the CSPG biosynthetic molecule *Chsy1* was significantly increased in subjects with SUD ($p < 0.05$; adjusted for significant effects of tissue pH) and in subjects with comorbid SUD and MDD ($p < 0.0001$; adjusted for significant effects of tissue pH and duration of AUD), while patients with MDD did not meet significance in any direction. Error bars are mean ± SEM.

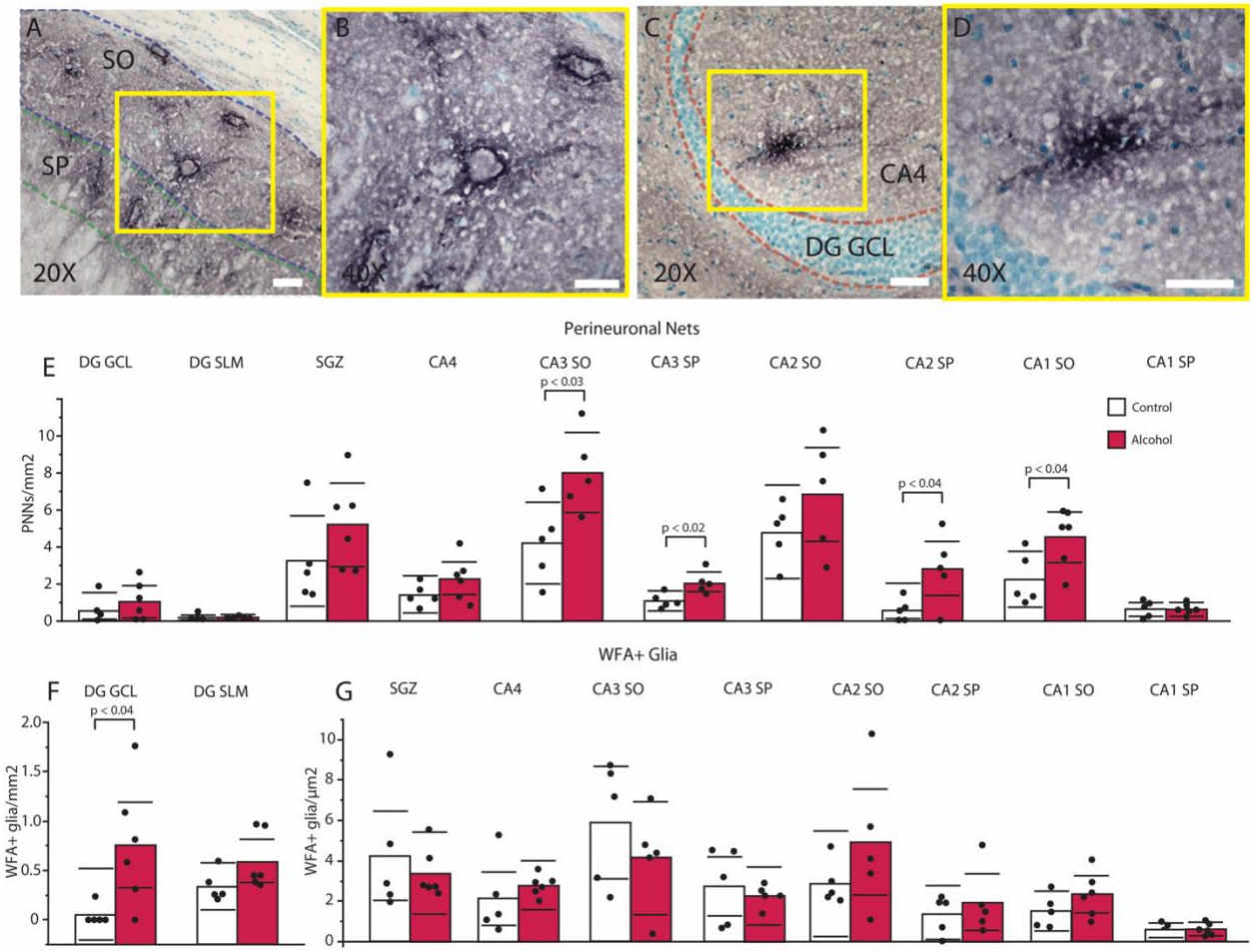

Figure 4. *Chronic alcohol self-administration increases PNN densities throughout the hippocampus of rhesus monkeys.* Abbreviations: DG GCL, granule cell layer of the dentate gyrus; SLM, stratum lacunosum moleculare; SGZ, subgranular zone; CA, cornu ammonis; SO, stratum oriens; SP, stratum pyramidale. (A) Representative microscopy of PNNs labeled with WFA in CA1 SO, scalebar = 50 µm. (B) Inset of Figure 4A at 40× magnification, scalebar = 30 µm. (C) Representative microscopy of a WFA-labeled glial cell proximal to the DG GCL, scalebar = 50 µm. (D) Inset of Figure 4C at 40× magnification, scalebar = 50 µm. (E) Comparisons of PNN densities throughout the hippocampus between control (white bars) and monkeys with chronic alcohol self-administration (red bars). (F) Comparison of WFA-glia densities in the DG GCL and DG SLM between control and monkeys with chronic alcohol self-administration. (G) Comparison of WFA-glia densities in the SGZ and CA nuclei of the hippocampus between control and monkeys with chronic alcohol self-administration.

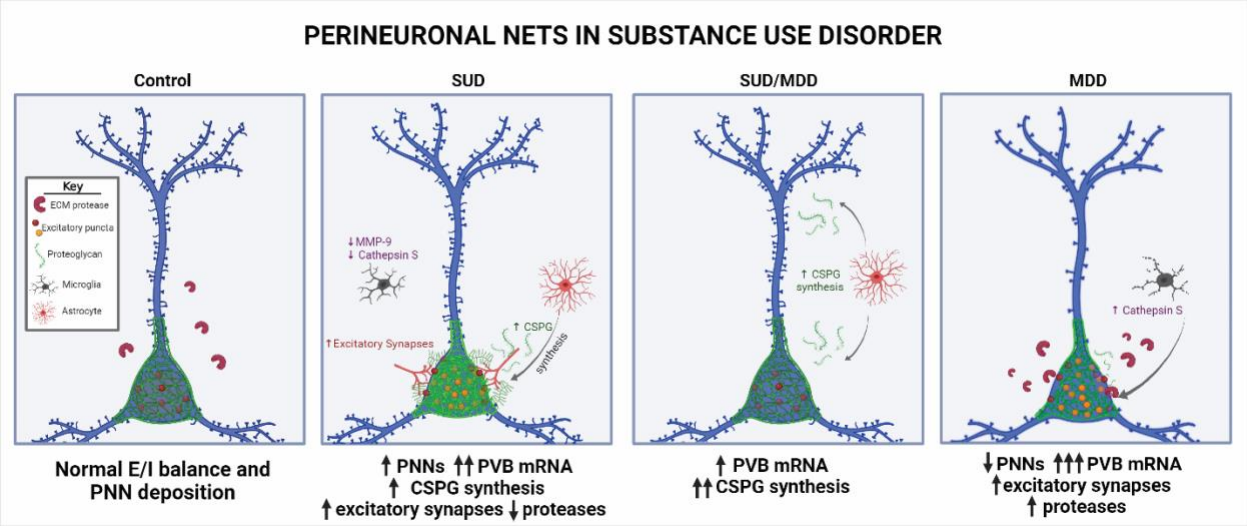

Figure 5. *Summary diagram of proposed ECM and synaptic alterations in the hippocampus of subjects with SUD with or without comorbid MDD.* Panels providing visual depictions of pathological observations from the present study. Numbers of arrows describe the intensity of changes compared to the other diagnostic groups, and a key is provided within the control panel to characterize the graphics used within the figure. Created with BioRender.com.